Parameters Calculation of Asymmetrical CPW-DGS

Zhongliang Deng, Xubing Guo*, Hao Wei, and Jun Gan

Abstract—In this paper, an analytical method of capacitance and characteristic impedance is proposed, which is for asymmetrical coplanar waveguide with defected ground structure (ACPW-DGS). The capacitance equivalent model of ACPW-DGS is established. Using conformal mapping method and first category of incomplete elliptic integrals $F(\varphi, k)$, the closed-form expressions of capacitance and characteristic impedance are obtained for the first time. Computed results match the simulated ones well.

1. INTRODUCTION

Coplanar waveguide (CPW) for the design of monolithic microwave integrated circuits (MMICs) has obtained increasing popularity [1], owing to its attractive features such as easy insertion of shunt or series active devices, low-frequency dispersion, and low substrate dependence [2]. Symmetrical CPW structures have been studied in many aspects such as capacitance, characteristic impedance, and equivalent circuits [3–6]. Electromagnetic field distribution of asymmetrical CPW with conductor backing has also been studied by Fang and Wang [7, 8]. However, little work, to date, has been done in asymmetrical CPW with defected ground structure (ACPW-GDS), which plays an important role in the design of resonators [9], filters [10], phase shifters, antennas [11] and other devices. Knorr and Kuchler analyzed slots and coplanar strips by using spectral domain method and Galerkin's method [12]. Davies and Mirshekar-Syahkal studied coplanar transmission line with multilayer substrate with similar method [13]. The structures of slots and coplanar strips are similar to CPW, but the results in [12, 13] are only appropriate for regular geography of symmetrical signal line and ground without defected structures. Spectral domain method is derived from Maxwell equations and Fourier transform. Its procedures are complicated, and its results depend on corresponding boundary condition. Furthermore, Galerkin's method is a numerical method. Its accuracy is determined by basis function. Depending on EM field distribution, choosing a basis function is very hard. What is worse, spectral domain method cannot obtain analytical solution and closed-form expressions of capacitance and characteristic impedance. Zhang et al. [14] presented the results of a symmetrical CPW with a symmetrical defected structure in signal line. To date, the research of ACPW-GDS has not been reported in available literatures. Obviously, the capacitance and characteristic impedance are easily affected by DGS, but those aforementioned methods cannot well solve the parameters of ACPW-GDS.

In this paper, the capacitance and characteristic impedance of ACPW-GDS are obtained by using conformal mapping method, and the analytical solution of ACPW-GDS is achieved for the first time. Compared to spectral domain method, this procedure is concise, and it is unnecessary to use numerical method. The main contributions of this paper are: (a) the capacitance equivalent model of ACPW-DGS is established; (b) first category of incomplete elliptic integrals $F(\varphi, k)$ is applied to calculate the characteristics parameters; (c) the analytical solution for capacitance and characteristic impedance of ACPW is obtained for the first time. Finally, FEM simulation results are used to verify accuracy of the analytical solution, and the FEM simulated and analytical results show a good agreement.

2. ANALYSIS OF CAPACITANCE EQUIVALENT MODEL AND CHARACTERISTIC IMPEDANCE

The physical structure of ACPW-DGS with finite height and width ground is shown in Fig. 1(a), and the thickness of the metal layer is ignored. It is assumed that the air-dielectric interfaces, where all the conductors are located, can be dealt with as perfect magnetic walls. The side view of ACPW-DGS along dashed line MN is shown in Fig. 1(b).
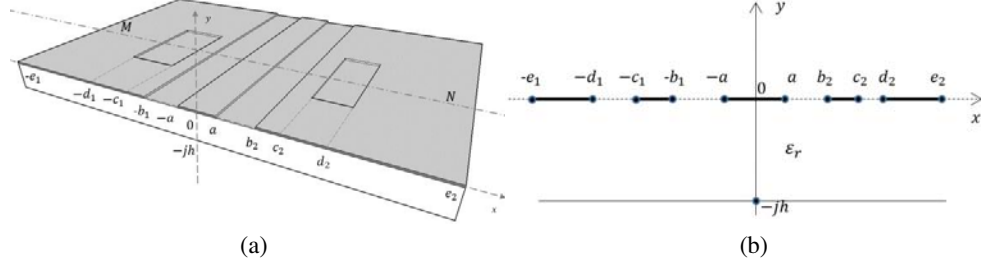
Figure 1. Physical structure and side view of ACPW-DGS: (a) physical structure; (b) the side view of ACPW-DGS along MN.

It has been shown [15] that in any transmission line the propagation characteristics can be formulated in terms of capacitance per unit length. The general capacitance equivalent model is shown in Fig. 2(a). Under the quasi-TEM assumption, these capacitances may be expressed in terms of a capacitance matrix. The capacitance matrix of the configuration shown in Fig. 2(a) is defined as [16]

$$
\begin{pmatrix} Q_1 \\ Q_2 \\ Q_3 \end{pmatrix} = \begin{pmatrix} C_1 & -C_{L1} & -C_{LR} \\ -C_{L1} & C_{L2} + C_{R2} & -C_{R1} \\ -C_{LR} & -C_{R1} & C_2 \end{pmatrix} \begin{pmatrix} V_1 \\ V_2 \\ V_3 \end{pmatrix} \tag{1}
$$

where V_i and $Q_i (i = 1, 2, 3)$ are, respectively, the potentials and total charges on the conductors shown in Fig. 2(a). However, on account that conductors ① and ② have the same potentials as ground plane shown in Fig. 2(b), only C_{L1}, C_{L2}, C_{R1} and C_{R2}, which will be calculated in this paper later, contribute to the characteristic impedance of ACPW-GDS.
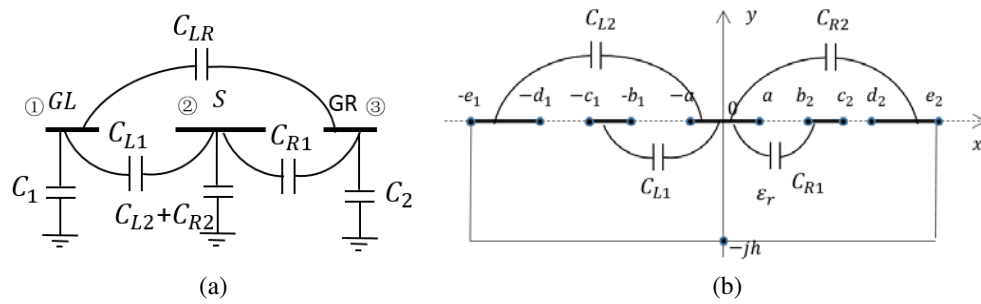
Figure 2. ACPW-DGS and capacitance model: (a) capacitance model of ACPW-DGS; (b) capacitances contributed to the characteristic impedance of ACPW-DGS.

The capacitance per unit length of the structure consists of two parts. Partial capacitances can be considered as air-filled spaces above and below the metallayer in the absence of dielectric layers and denoted by C_{R1-air}, C_{R2-air}, C_{L1-air}, and C_{L2-air}, respectively. The other capacitances are due to substrate with equivalent relative permittivity $(\varepsilon_r - 1)$ and denoted by C_{R1-di}, C_{R2-di}, C_{L1-di}, and C_{L2-di}, respectively.

$$
\begin{cases} C_{R1} = C_{R1-air} + C_{R1-di} \\ C_{R2} = C_{R2-air} + C_{R2-di} \end{cases} \quad \begin{cases} C_{L1} = C_{L1-air} + C_{L1-di} \\ C_{L2} = C_{L2-air} + C_{L2-di} \end{cases} \tag{2}
$$

The total capacitance C_{total} contributing to the characteristic impedance of ACPW-DGS is defined as

$$C_{total} = C_{R1} + C_{R2} + C_{L1} + C_{L2} \tag{3}$$

Characteristic impedance of ACPW-DGS is as follows, according to [17]

$$Z_0 = \frac{1}{c\sqrt{C_{total}C_{air}}} \tag{4}$$

where $C_{air} = C_{R1-air} + C_{R2-air} + C_{L1-air} + C_{L2-air}$, and capacitances C_{R1-air}, C_{R2-air}, C_{L1-air}, C_{L2-air}, C_{R1-di}, C_{R2-di}, C_{L1-di} and C_{L2-di} will be calculated in this paper later, respectively.

3. CALCULATIONS OF CAPACITANCE AND CHARACTERISTIC IMPEDANCE

In the right-hand half plane as shown in Fig. 3(a), only the first quadrant has to be considered on account of symmetry when we evaluate the capacitance of air-filled spaces, and only the fourth quadrant has to be considered when we calculate the capacitance of dielectric-filled region with relative permittivity $(\varepsilon_r - 1)$. Figs. 3(b) and 3(c) correspond to t-plane and s-plane mappings from Fig. 3(a), respectively. The z-plane first quadrant in Fig. 3(a) is transferred to t-plane through function $t = z^2$. After the transformation, the calculation region all located in the upper half t-plane. The s-plane is transferred from dielectric region in z-plane fourth quadrant by applying function $s = \cosh^2(\pi z/2h)$. Fig. 3(d) is W-plane mapping from Figs. 3(b) and 3(c) by using Schwarz transformation. Corresponding points in different planes are denoted by the same serial number, respectively.
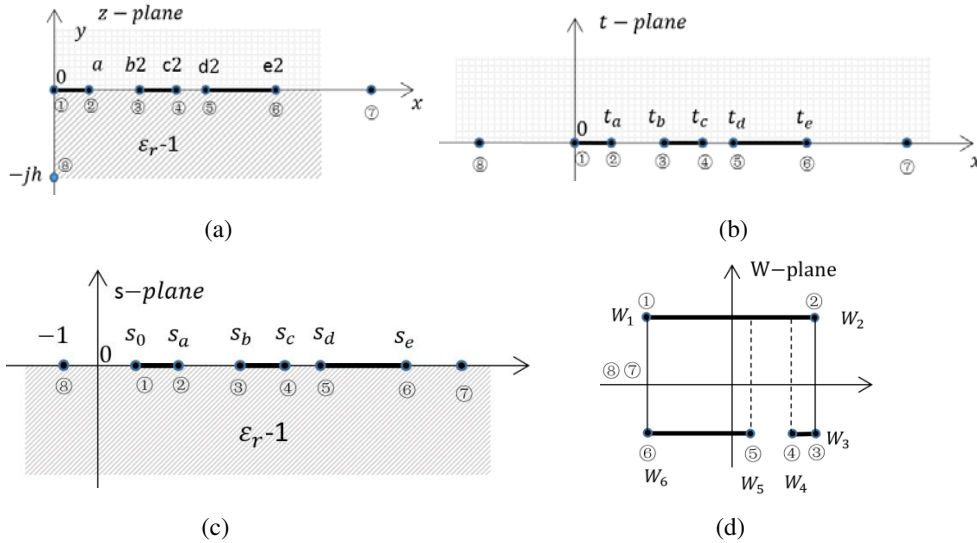
Figure 3. (a) The side view of CPW-DS; (b) first quadrant mapped to t-plane; (c) fourth quadrant with dielectric mapped to s-plane; (d) Fig. 3(b) and (c) mapped to W-plane.

3.1. Air Layer Analysis

The air layer is analyzed by using conformal mapping method. The capacitance and characteristic impedance closed-form expressions are obtained by applying Schwarz transformation, first category of incomplete elliptic integrals $F(\varphi, k)$ and complete elliptic integrals $K(k)$. From Schwarz polygon transformation, the relationship between t- and W-planes is expressed as

$$w = A \int_0^t \frac{d\tau}{\sqrt{\tau(\tau - t_a)(\tau - t_b)(\tau - t_e)}} \tag{5}$$

$$t_0 = 0 \quad t_a = a^2 \quad t_b = b_2^2 \quad t_c = c_2^2 \quad t_d = d_2^2 \quad t_e = e_2^2$$

Constant parameter A which acts as scale factor of the length in W-plane is assumed 1 without loss of generality [15]. The length of $\overline{W_6W_3}$ in Fig. 2(d) is

$$\overline{W_6W_3} = \int_{t_b}^{t_e} \frac{d\tau}{\sqrt{\tau(\tau - t_b)(\tau - t_e)(\tau - t_a)}} = \int_0^1 \frac{d\xi}{\sqrt{(1 - \xi^2)(1 - k_a^2\xi^2)}} = g_aK(k_a) \qquad (6)$$

Some parameters are defined as follows

$$r = \frac{t_e(t - t_b)}{(t_e - t_b)t} = \xi^2, \quad g_a = \frac{2}{\sqrt{(t_e - t_0)(t_b - t_a)}}, \quad k_a^2 = \frac{t_a(t_b - t_a)}{t_e(t_e - t_a)}$$

The same method is applied to calculate $\overline{W_3W_2W_4W_3}$ and $\overline{W_5W_3}$

$$\begin{cases} \overline{W_4W_3} = \int_{\beta_b}^{\beta_c} \frac{d\xi}{\sqrt{(1 - \xi^2)(1 - k_a^2\xi^2)}} = g_aF(k_a, \arcsin\beta_c) \\ \overline{W_5W_3} = \int_{\beta_b}^{\beta_d} \frac{d\xi}{\sqrt{(1 - \xi^2)(1 - k_a^2\xi^2)}} = g_aF(k_a, \arcsin\beta_d) \\ \overline{W_3W_2} = g_aK(k_a') \end{cases} \qquad (7)$$

$$k_a' = \sqrt{1 - k_a^2} \quad \beta_b = 0, \quad \beta_c = \sqrt{\frac{t_e(t_c - t_b)}{t_c(t_e - t_b)}}, \quad \beta_d = \sqrt{\frac{t_e(t_d - t_b)}{t_d(t_e - t_b)}}$$

The capacitance is calculated according to parallel capacitor formula and symmetry property [18]

$$\begin{cases} C_{R1-air} = 2\varepsilon_0\frac{(\overline{W_5W_3} + \overline{W_4W_3})}{2\overline{W_3W_2}} = \varepsilon_0\frac{[F(k_a, \arcsin\beta_d) + F(k_a, \arcsin\beta_c)]}{K(k_a')} \\ C_{R2-air} = 2\varepsilon_0\frac{\overline{W_6W_3} - \overline{W_5W_3}}{\overline{W_3W_2}} = 2\varepsilon_0\frac{[K(k_a) - F(k_a, \arcsin\beta_d)]}{K(k_a')} \end{cases} \qquad (8)$$

Applying conformal mapping method, capacitances C_{L1-air} and C_{L2-air} in the left half z-plane can be determined by using similar formulas shown in Table 1, but the coordinates of corresponding points should use left half z-plane.

3.2. Dielectric Layer Analysis

The dielectric region in the z-plane is first transformed onto the s-plane through the mapping function $s = \cosh^2(\pi z/2h)$, and corresponding points in s-plane are

$$s_0 = 1, s_a = \cosh^2\left(\frac{\pi a}{2h}\right), \ s_b = \cosh^2\left(\frac{\pi b_2}{2h}\right), \ s_c = \cosh^2\left(\frac{\pi c_2}{2h}\right), \ s_d = \cosh^2\left(\frac{\pi d_2}{2h}\right), \ s_e = \cosh^2\left(\frac{\pi e_2}{2h}\right)$$

The side lengths of the rectangle after transform are expressed as

$$\overline{W_6W_3} = g_dK(k_d), \ \overline{W_3W_2} = g_dK(k_d'), \ \overline{W_4W_3} = g_dF(k_d, \arcsin\eta_c), \ \overline{W_5W_3} = F(k_d, \arcsin\eta_d)$$

$$\beta_b = 0, \quad \beta_c = \sqrt{\frac{(s_e - s_0)(s_c - s_b)}{(s_e - t_b)(s_c - s_0)}}, \quad \beta_d = \sqrt{\frac{(s_e - s_0)(s_d - s_b)}{(s_e - t_b)(s_d - s_0)}}$$

$$g_a = \frac{2}{\sqrt{(s_e - s_0)(s_b - s_a)}} \quad k_d^2 = \frac{(s_e - s_b)(s_a - s_0)}{(s_b - s_a)(s_e - s_0)}, \quad k_d' = \sqrt{1 - k_d^2}$$

The closed-form expressions of C_{R1-di} and C_{R2-di} are expressed as follows

$$\begin{cases} C_{R1-di} = \varepsilon_0(\varepsilon_r - 1)\frac{1}{2}\frac{\overline{W_5W_3} + \overline{W_4W_3}}{\overline{W_3W_2}} = \varepsilon_0(\varepsilon_r - 1)\frac{[F(k_d, \arcsin\eta_d) + F(k_d, \arcsin\eta_c)]}{2K(k_a')} \\ C_{R2-di} = \varepsilon_0(\varepsilon_r - 1)\frac{\overline{W_6W_5}}{\overline{W_3W_2}} = \varepsilon_0(\varepsilon_r - 1)\frac{[K(k_d) - F(k_a, \arcsin\beta_d)]}{K(k_a')} \end{cases} \qquad (9)$$

Applying similar conformal mapping procedures, capacitances C_{L1-di} and C_{L2-di} in the left half z-plane can be determined by using similar formulas, but the coordinates of corresponding points should be replaced by points in the left half z-plane. The formulas of capacitance in left half z-plane are shown in Table 1. Thus, the capacitances are obtained by foregoing expressions, and characteristic impedance is obtained by Equation (4).

Table 1. The formulas of capacitance in the left half z-plane.

Capacitance formulas	Corresponding parameters setting
$C_{L1-air} = \varepsilon_0 \frac{[F(k_a,\arcsin\beta_d)+F(k_a,\arcsin\beta_c)]}{K(k'_a)}$ $C_{L2-air} = 2\varepsilon_0 \frac{[K(k_a)-F(k_a,\arcsin\beta_d)]}{K(k'_a)}$	$t_0 = 0,\ \ t_a = a^2,\ t_b = b_1^2,$ $t_c = c_1^2,\ t_d = d_1^2,\ \ t_e = e_1^2$
$C_{L1-di} = \frac{\varepsilon_0(\varepsilon_r-1)[F(k_d,\arcsin\eta_d)+F(k_d,\arcsin\eta_c)]}{2K(k'_a)}$ $C_{L2-di} = \frac{\varepsilon_0(\varepsilon_r-1)[K(k_d)-F(k_a,\arcsin\beta_d)]}{K(k'_a)}$	$s_0 = 1,\ \ \ s_a = \cosh^2\left(\frac{\pi a}{2h}\right),\ s_b = \cosh^2\left(\frac{\pi b_1}{2h}\right),$ $s_c = \cosh^2\left(\frac{\pi c_1}{2h}\right), s_d = \cosh^2\left(\frac{\pi d_1}{2h}\right),$ $s_e = \cosh^2\left(\frac{\pi e_1}{2h}\right)$

3.3. Some Important Results of Degenerated Situations

According to the above capacitance evaluating procedure, some important results of degenerated situations for ACPW-DGS can be summarized as shown in Table 2. By replacing corresponding points coordinates, similar formulas of capacitance can be expressed as Formulas (8) and (9).

Table 2. Some important results of degenerated situations for ACPW-DGS.

Shape of structure	Coordinates setting	Shape of structure	Coordinates setting
	$b_1 = b_2,\ c_1 = c_2$, $d_1 = d_2, e_1 = e_2$ (symmetrical structure)		$b_2 = c_2 = d_2$ (defected structure in single half plane)
	$b_1 = c_1 = d_1,$ $c_2 < 0,\ d_2 < a$ (defected structure in signal conductor)		$b_1 = c_1,\ b_2 = c_2$ (wing shape defected ground structure)
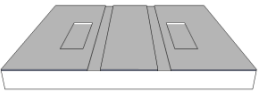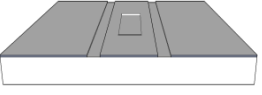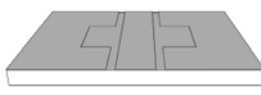
4. NUMERICAL RESULTS VERIFICATION

The simulation structure based on a substrate FR-4, with relative permittivity of 4.8, thickness of 1.6 mm and tangent angle loss of 0.017, is shown in Figs. 4(b), 4(c) and 4(d). Fig. 4(a) is an equivalent circuit of those structures. The equivalent circuit is applied to evaluate the characteristic impedance of ACPW-GDS and compared with the results from Formula (4). The procedure of this process consists of three steps. First, obtaining the capacitance and characteristic impedance from Formulas (8), (9) and (4); second, getting simulation results of input impedance from FEM method; third, calculating characteristic impedance from Formula (10) and compared to the calculation results.
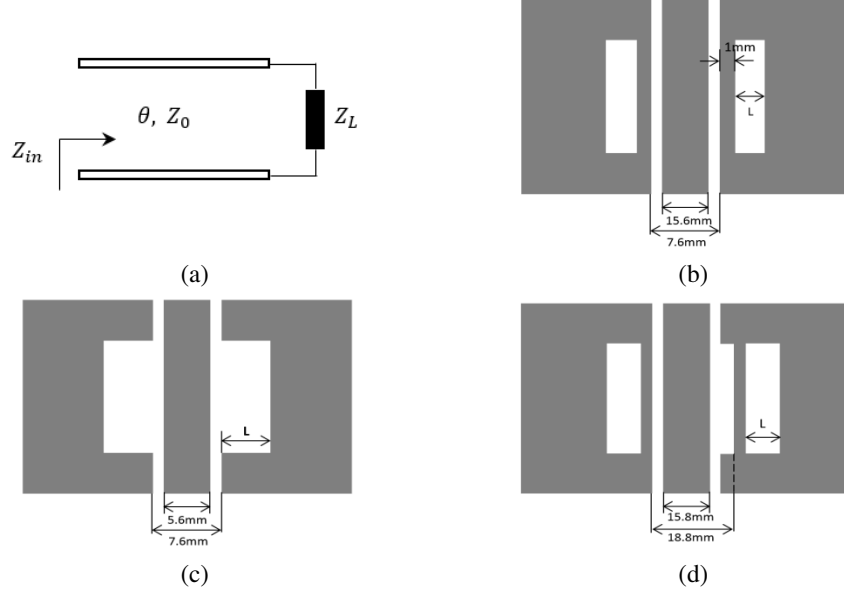
Figure 4. The simulation structure and its equivalent circuit: (a) the equivalent circuit of Figs. 4(b), 4(c) and 4(d); (b) physical structure I; (c) physical structure II; (d) physical structure III.

$$Z_{0S} = \frac{Z_L - Z_{in} - \sqrt{(Z_{in} - Z_L)^2 - 4Z_{in}Z_L \tan^2 \theta}}{2j \tan \theta} \tag{10}$$

where $\theta = 2\pi l/\lambda_g$, $l = 32$ mm, $f_0 = 0.675$ GHz. According to the dimension of the structure shown in Figs. 4(b), 4(c) and 4(d), parameters k_a, k_d, C_{R1}, C_{R2}, C_{L1}, C_{L2}, C_{total} and Z_0 can be calculated according to variable L marked in Fig. 4, respectively. The data of C_{air}, C_{total} and Z_0 are shown in Table 3.

Table 3. Data of capacitance and characteristic impedance of different structure dimension.

Results L (mm)	C_{tota} (pF)			C_{air} (pF)			Z_0 (Ω)			Z_{0S} (Ω)		
	I	II	III	I	II	III	I	II	III	I	II	III
0.5	84.0	74.1	74.7	42.6	46.8	44.3	55.7	56.6	57.9	56.3	57.0	58.3
1	82.9	71.1	73.4	41.5	40.3	43.1	56.8	62.3	59.3	57.1	62.4	59.6
1.5	82.1	68.3	72.2	40.7	36.1	41.8	57.7	67.1	60.7	58.0	67.2	61.1
2	81.3	65.8	71.3	39.8	33.2	40.9	58.6	71.3	61.7	59.0	71.7	62.3
2.5	80.6	63.3	70.5	39.1	31.0	40.2	59.4	75.2	62.6	60.1	75.9	63.4
3	79.9	61.3	69.8	38.5	29.1	39.4	60.1	78.9	63.6	60.9	79.8	64.5
3.5	79.4	59.7	69.2	38.0	27.5	38.8	60.7	82.3	64.3	61.6	83.1	65.3
4	79.1	57.9	68.6	37.7	26.2	38.3	61.0	85.6	65.0	62.3	87.1	66.1
4.5	78.8	56.4	68.1	37.4	25.1	37.8	61.4	88.6	65.7	62.8	89.6	66.8
5	78.7	54.6	67.8	37.3	24.3	37.4	61.5	91.5	66.2	63.5	92.4	67.5

Figures 5(a)–5(c) show the relationship of C_{air}, C_{total} and Z_0 with respect to length of L as marked in Figs. 4(b)–4(c). In general, capacitances C_{air} and C_{total} decrease as the length of L increasing from 0 to 5 mm, and structure II (shown in Fig. 4(c)) has a steep decrease. Fig. 5(c) shows the relationship among Z_0 (calculated), Z_{0S} (simulated) and length of L. Z_0 changes almost 10.41% of structure I, 61.66% of structure II and 14.34% of structure III when L changes from 0.5 mm to 5 mm, respectively.
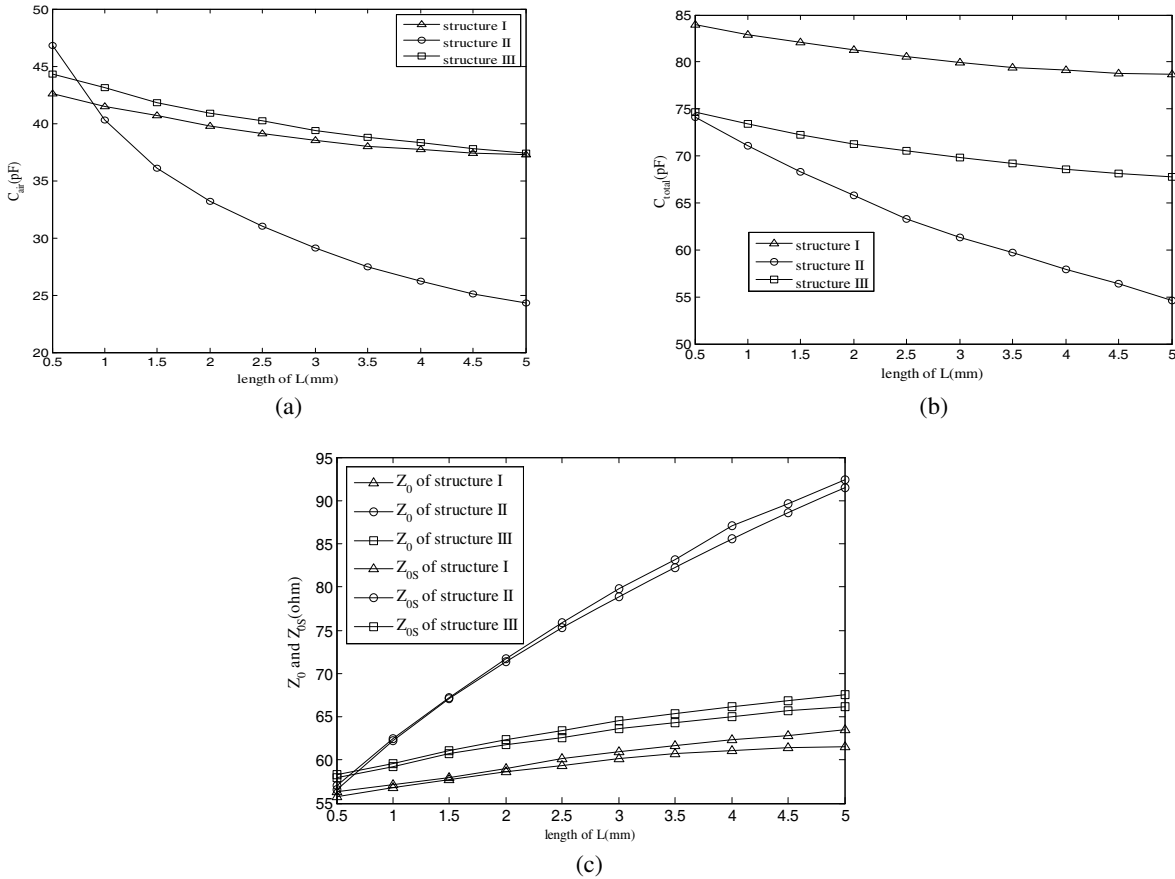
Figure 5. The relationship of C_{air}, C_{total} and Z_0 with respect to length of L: (a) C_{air}; (b) C_{total}; (c) Z_0 and Z_{0S}.

Apparently, the capacitance and characteristic impedance of structures I and III are not sensitive to the length of L. These results show a good agreement between Z_0 and Z_{0S}, which means that the method presented in this paper is effective. It is clear that all the curves exhibit an exponentially decaying character with respect to the length of L, because the electric field density also has an exponentially decaying character. The little difference between Z_0 and Z_{0S} was caused by errors in calculation and simulation.

5. CONCLUSION

ACPW-GDS is analyzed in this paper, and capacitance of unit length and characteristic impedance are obtained by conformal mapping method. The closed-expressions of capacitance and characteristic impedance are formulated by using the first category of complete and incomplete elliptic integrals $F(\varphi, k)$, $K(k)$. Analytical and numerical results show a good agreement, which shows that this method is a good way to calculate the parameters of ACPW-GDS.

REFERENCES

1. Lim, J., C. Kim, D. Ahn, Y. Jeong, and S. Nam, "Design of low-pass filters using defected ground structure," *IEEE Trans. Microw. Theory Tech.*, Vol. 53, No. 8, 2539–2545, 2005.
2. Simons, R., *Coplanar Waveguide Circuits, Components, and System*, John Wiley & Sons, Ann Arbor, 2001.

3. Mao, S.-G. and M.-S. Wu, "Design of artificial lumped-element coplanar waveguide filters with controllable dual passband responses," *IEEE Trans. Microw. Theory Tech.*, Vol. 56, No. 7, 1684–1692, 2008.

4. Guo, X. L., C. Xu, G. A. Zhang, Z. J. Zhang, H. H. Yin, and Z. L. Wang, "Tunable low-pass MEMS filter using defected ground structures (DGS)," *Solid-State Electronics*, Vol. 94, No. 6, 28–31, 2014.

5. Wen, C. P., "Coplanar waveguide: A Surface strip transmission line suitable for non-reciprocal gyromagnetic device application," *IEEE Trans. Microw. Theory Tech.*, Vol. 18, No. 17, 1087–1090, 1969

6. Zhu, L. and K. Wu, "Characterization of finite-ground CPW reactive series-connected elements for innovative design of uniplanar M(H)MICs," *IEEE Trans. Microw. Theory Tech.*, Vol. 50, No. 2, 549–557, Feb. 2002.

7. Fang, S.-J. and B.-S. Wang, "Analysis of asymmetric coplanar waveguide with conductor backing," *IEEE Trans. Microw. Theory Tech.*, Vol. 47, No. 2, 238–240, 1999.

8. Fang, S., "Study on the characteristic and field pattern of asymmetric coplanar waveguides," Doctoral Thesis, Dalian Maritime University, Feb. 2001.

9. El-Shaarawy, H. B., F. Coccetti, and R. Plana, "Novel reconfigurable defected ground structure resonator on coplanar waveguide," *IEEE Trans. Antennas Propag.*, Vol. 58, No. 11, 3622–3628, Nov. 2010.

10. Lim, J.-S., C.-S. Kim, and D. Ahn, "Design of low-pass filters usingdefected ground structure," *Microw. Theory Tech.*, Vol. 53, No. 8, 2539–2545, Aug. 2005

11. Tariq, A. and H. Ghafouri-Shiraz, "Frequency-reconfigurable monopole antennas," *IEEE Trans. Antennas Propag.*, Vol. 60, No. 1, 44–50, Jan. 2012.

12. Knorr, J. and K.-D. Kuchler, "Analysis of coupled slots and coplanar strips on dielectric substrate," *IEEE Trans. Microw. Theory Tech.*, Vol. 23, No. 7, 541–547, 1975.

13. Davies, J. B. and D. Mirshekar-Syahkal, "Spectral domain solution of arbitrary coplanar transmission line with multilayer substrate," *Microw. Theory Tech.*, Vol. 25, No. 10, 143–146, 1977.

14. Zhang, N., et al., "Analytical solution for capacitance and characteristic impedance of CPW with defected structures in signal line," *Progress In Electromagnetics Research Letters*, Vol. 54, 79–84, 2015.

15. Liang, C., *Concise Microwave*, 163–164, Higher Education Press, 2006.

16. Cheng, K.-K. M., "Characteristic parameters of symmetrical triple coupled CPW lines," *Electronics Letters*, Vol. 33, No. 8, 685–686, Apr. 1997.

17. Dib, N., "Comprehensive study of CAD models of several coplanar waveguide (CPW)discontinuities," *IEE Proc. Microw. Antennas Propag.*, Vol. 152, No. 2, 69–76, Apr. 2005.

18. Cheng, K.-K. M., "Analytical formula for calculating the coupling characteristics between parallel coplanar lines," *Electronics Letters*, Vol. 32, No. 13, 120–1209, 1996.